Stanford Exploration Project, Report 120, May 3, 2005, pages 217–237

Stanford Exploration Project, Report 120, May 3, 2005, pages 217–237

Focusing-effect AVO/AVA: overview of results and assessment of problems

Ioan Vlad[1]

ABSTRACT

Small-scale heterogeneities in the Earth produce visible focusing of seismic wavefield amplitudes with offset, but minimal variations in traveltimes. These effects are called Focusing-Effect AVO (FEAVO) or AVA (FEAVA) for avoiding confusion with lithology-caused AVO/AVA. FEAVO/FEAVA is not an unpredictable phenomenon that occurs at random. It appears in a number of well-defined geological settings, it can be modeled with appropriate precautions, it can be identified by its spatially predictable patterns, and can be removed in a manner that takes into account the specific physics involved. This paper summarizes work published over the course of several years in seven different SEP reports, providing an overview of the results obtained up to date and an assessment of the most critical problems to be solved.

INTRODUCTION

Amplitudes of reflected seismic waves have concerned geophysicists since the beginnings of the profession (Gutenberg, 1936). However, until the advent of digital recording in the late sixties, efforts in this direction were mainly theoretical (Bortfeld, 1961). "Bright-spot" technology started a first wave of applied amplitudes research in the early seventies (Craft, 1973), and the emergence of Amplitude Variation with Offset (AVO) techniques (Shuey, 1985) assured amplitudes a solid place in the geophysicist's toolbox. The line of research to which this paper belongs was started by Kjartansson (1979).

Kjartansson observed that zones with amplitudes too large to be explained by lithological contrasts at the reflector or by tuning were correlated in a predictable way in the prestack data volume, and he provided a conceptual explanation for it. I will call these phenomena Focusing-Effect AVO/AVA (FEAVO/FEAVA).[2] The section that follows after the Introduction will describe them in detail. The important thing to note, and the motivation for this work, is that: (1) those anomalous amplitudes are caused by wavefield focusing through velocity or absorption lenses, (2) that they impede proper AVO/AVA analysis or any other amplitude analysis techniques, and that therefore (3) they should be removed from the seismic image. Work on this subject has been published sporadically, especially at SEP, ever since Kjartansson's

[1]**email:** nick@sep.stanford.edu

[2]The name FEAVA will be used only when referring specifically to the angle domain.

paper. The most recent publications related to this topic are Vlad and Biondi (2002), Vlad et al. (2003a), and Vlad (2002; 2003; 2004a; 2004b; 2005). While these articles dealt with highly specific details, the material that follows will provide an overview of the current state of knowledge about FEAVO and its removal, with assessments of the problems that remain to be solved, in highlighted paragraphs.

FEAVO DESCRIPTION

Geologic setting

FEAVO effects are caused by focusing through velocity or absorption heterogeneities smaller than the Fresnel zone (Spetzler et al., 2004) – too small to be resolved by velocity analysis methods currently employed in production settings, too small to send the energy outside the aperture of the seismic survey, but not so small and sharp that they would simply cause a diffraction. This means roughly "a few tens of meters". White et al. (1988) shows analytically that it is more likely that the interfaces are smooth rather than sharp. Highly visible FEAVO effects appear easily in the presence of velocity contrasts as small as 2%, and no absorption (Vlad, 2004a). Examples of such heterogeneities include:

(1) Irregular interfaces between spatially extended media with different velocity and/or absorption characteristics: (a) channels on the sea bottom caused by currents, former rivers, or glaciers; (b) positive landforms on sea bottom such as moraines (North Sea); (c) Irregular thickness of permafrost; (d) low-velocity eolian, fluvial or marine sediment covering karst features or other irregular erosion surfaces; (e) interfaces of plastic clay or salt bodies. In this case FEAVO can be hard to see because of the much more powerful illumination effects caused by interface undulations of a larger spatial wavelength than those which cause FEAVO.

(2) Small lenticular bodies of contrasting properties with the surrounding medium. They may be filled with gas, in which case absorption would play an important role. They can be small in all directions, as would be the case with filled peat bogs, or they can be elongated along one direction, such as gas sand-filled river channels (small in cross-section) or lenses formed by gas-liquid contact inside a fold associated with normal listric faulting, (left panel in Figure 1).

(3) Termination of a relatively thin layer of highly contrasting properties with the surrounding medium, either by tapering off stratigraphically (right panel in Figure 1), or by ending abruptly against a fault (Hatchell, 1999, 2000a,b). The latter case, illustrated by Figure 2, is interesting becayse it may occur much deeper (thousands of meters) than the previously described ones, and the bodies causing the FEAVO anomalies may have much sharper interfaces.

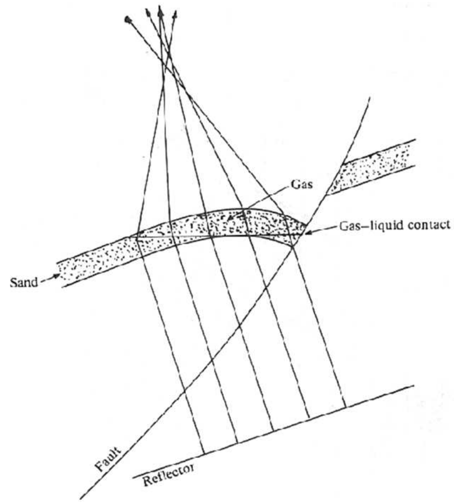

Figure 1: Examples of geologic settings which may cause focusing. From Sheriff and Geldart (1995). nick2-sheriff [NR]

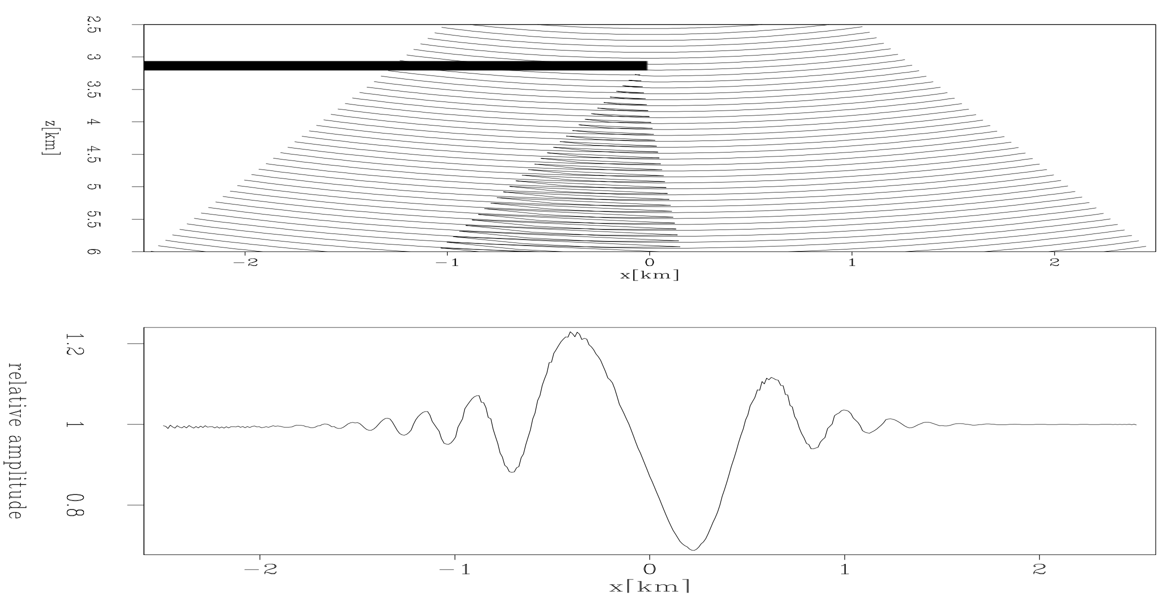

Figure 2: **Top:** Velocity model and isochrones for a shot at (0,0). The background is 1830m/s and the slab is 1647m/s. No absorption, pseudospectral two-way method. **Bottom:** The shot is downward continued through the velocity model with the slab and without the slab to simulate the seismograms that a horizontal strings of geophones would record at a depth of 6000m. At each *x* location, the plotted value is the ratio between the highest amplitude obtained at that location without the slab and with the slab. The end of the slab induces focusing. The dispersion is just a numerical effect. From Vlad and Tisserant (2004). nick2-g3_sep120 [CR]

Needed: realistic modeling of these FEAVO-causing geologic settings with a variety of plausible parameters (shape, size, depth, velocity, Q), in 2-D and 3-D, in order to estimate the range of parameters which results in FEAVO anomalies (source too small to be resolved by state-of-the-art velocity analysis methods used in production, yet too large and smooth to cause diffractions). This is a computationally-intensive task. The datasets obtained from modeling could be used as benchmarks for FEAVO detection and removal.

FEAVO effects in the data

The first sign of FEAVO that one may encounter in a dataset are subvertical streaks of alternating high and low amplitudes in constant-offset sections (left panel in Figure 3). At a closer inspection, the affected areas show traveltime departures from hyperbolicity as small as 2-3 ms (Carazzone et al., 1984) and as large as 20 ms (Kjartansson, 1979). An illustration of these effects is presented in the middle panel of Figure 3. The amplitudes in these areas may be easily three times larger than those in unaffected areas (White et al., 1988). The effects may be frequency-dependent and distort the wavelet (Stephens and Sheng, 1985; Vlad and Biondi, 2002).

Needed: modeling of purely-velocity and purely-absorption FEAVO, in order to investigate whether the frequency-dependent effects can serve to discriminate between FEAVO caused by absorption and that caused by velocity.

While the above-described effects are visible and are what started FEAVO research in the seventies, FEAVO's certain "signature" in the data domain (before migration) is the "Kjartansson V's". These shapes appear if we window a prestack 2-D line to roughly include the areas with anomalous amplitudes, then take the absolute value of each sample, *stack* the prestack dataset along the time axis and display the resulting midpoint-offset plot with an appropriate gain. "V" shapes become visible (right panel in Figure 3). This may not occur if the background velocity in the medium varies so strongly with midpoint as to distort these shapes too much.

The heuristic used by Kjartansson (1979) to explain the formation of the "V" shapes is presented in Figure 4. The "V" shapes are the result of stacking along the time axis surfaces which in constant velocity are described by

$$h = \frac{t}{t - t_a} \cdot |m - m_a| \qquad (1)$$

A form of this equation is given by Rocca and Toldi (1982), with a simpler proof of another form in Vlad (2002). h is the half offset, t is traveltime, m is midpoint, t_a and m_a are the location of the heterogeneity that causes the focusing. Figure 5 gives a better view of the path of the FEAVO effects through the prestack dataset. The shape resembles the bow of a capsized boat. Its slope becomes asymptotically vertical with time and the opening of the "V"s becomes asymptotically 45° as the traveltime to the focusing source becomes negligible. It is visible

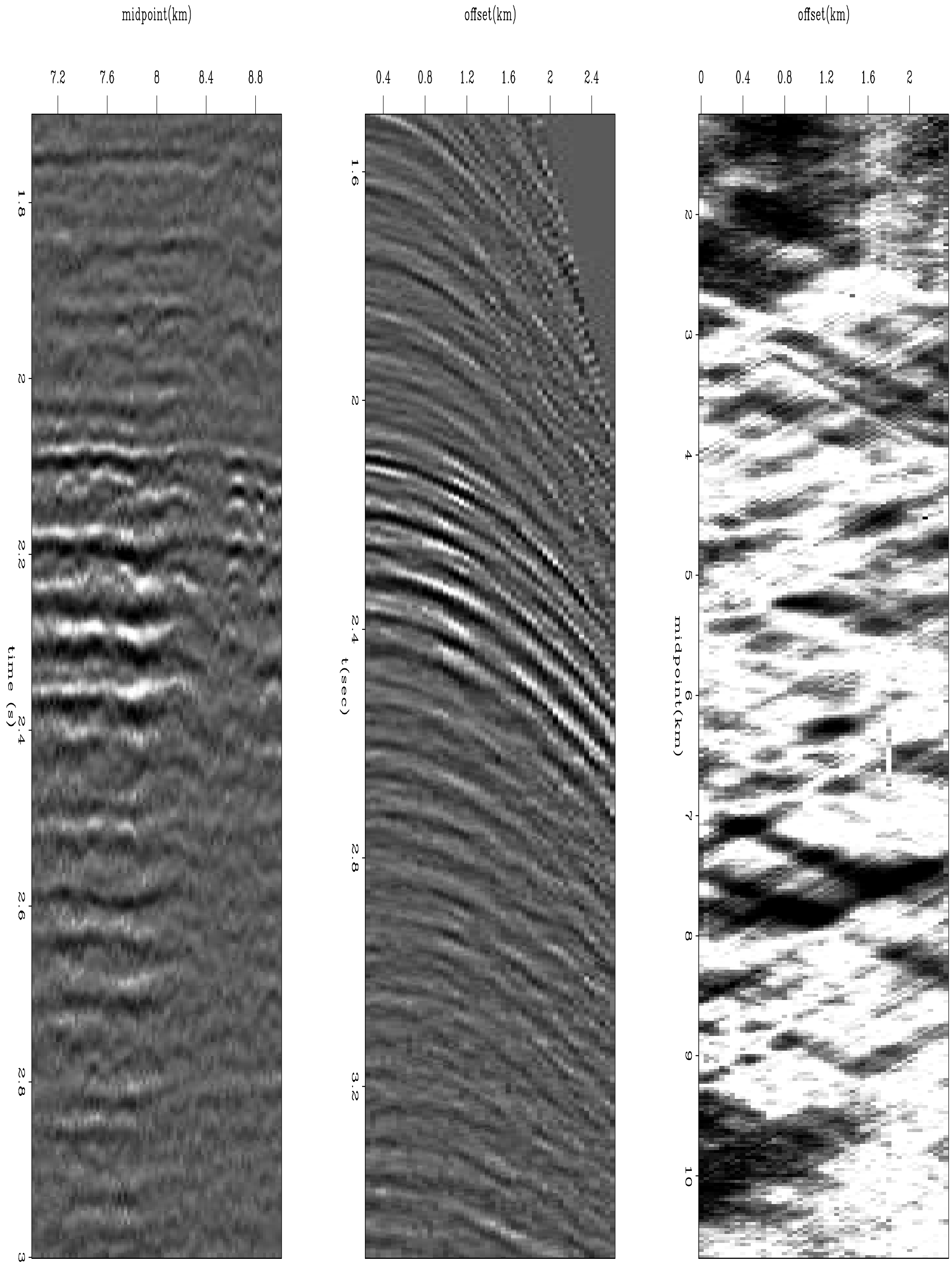

Figure 3: FEAVO in the data domain (before migration). Grand Isle dataset, also used by Vlad and Biondi (2002) **Left:** vertical amplitude streaks in constant-offset section. **Center:** Milisecond-sized departures from hyperbolicity. Most visible at 2.35s. **Right:** Kjartansson V's in the midpoint-offset space, after stacking the unsigned values along the time axis. nick2-new_prodef [ER]

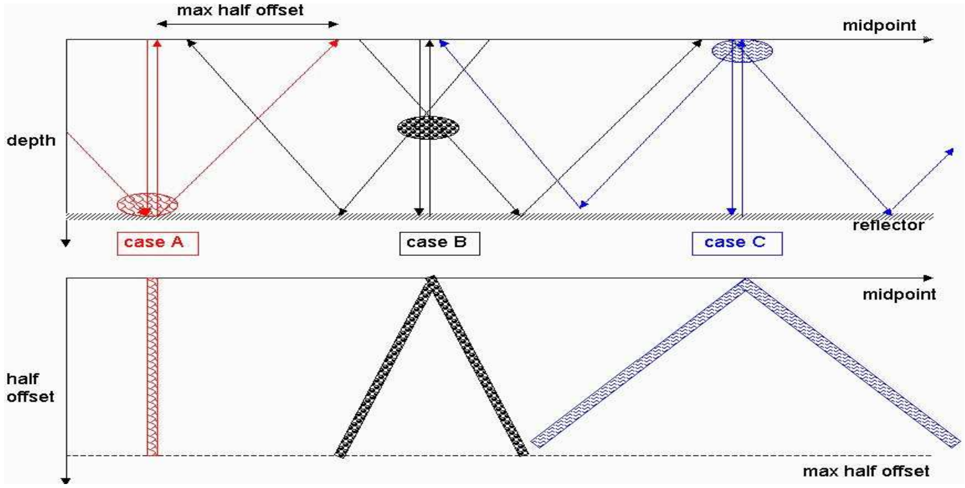

Figure 4: The physical explanation for the expression of FEAVO anomalies in midpoint-offset space Kjartansson "V"s. In the upper picture, the blobs are transmission anomalies and the arrows are raypaths for the zero offset and for the maximum offset recordings. For case A (anomaly on the reflector), only a single midpoint is affected, for all offsets. Case C (anomaly at the surface), is actually a static: its "footprint" is a pair of streaks slanting 45^o from the offset axis. Case B (in between) gives a pair of streaks with angles smaller than 45^o. From Vlad and Biondi (2002). nick2-vilus [NR]

now why stacking along the time axis a window in the middle of the prestack data volume would produce a "V".

A subtle, little-studied aspect of FEAVO effects is the distribution of the anomalous amplitudes when the anomaly paths described above intersect reflectors, for which I will use the name "FEAVO microstructure". Since an absorption-free, velocity-only "lens" conserves energy, any increase in amplitudes would have to be bordered by one or two shadow zones, and a decrease – by two illuminated zones. Finite-frequency wave theory predicts this for absorption-free media and ultrasonic experiments confirm it, as illustrated by Figure 4 of Spetzler et al. (2004). I am not aware of any equivalent studies for absorption. The existence or not of shadow/hightlight border zones for absorption is important because it may offer an avenue of discriminating between absorption-caused FEAVO and velocity-caused FEAVO, a key issue when trying to remove focusing with methods based on the physics of the phenomena (not just image processing).

Needed: A theoretic/numeric study of the magnitude of the shadow/highlight efects bordering FEAVO with parameters likely to be encountered in real exploration surveys, including absorption.

The polarity of the FEAVO on a reflector depends on the polarity of the velocity anomaly causing the FEAVO (negative or positive with respect to the background) and on the polarity of the reflector itself. The rightmost "V" in the bottom panel of Figure 8 illustrates the depen-

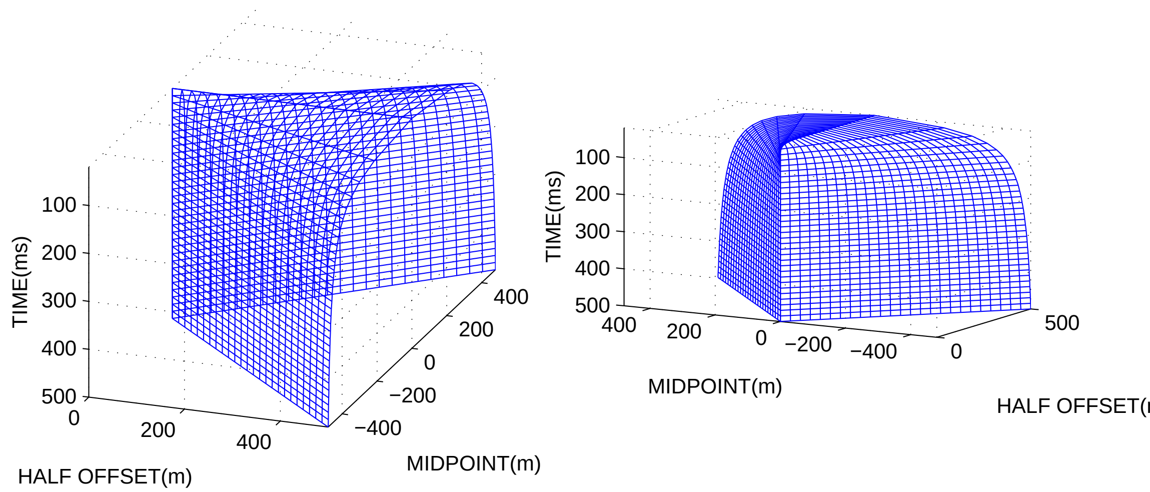

Figure 5: Path of FEAVO effects through the prestack data volume in constant velocity, flat reflectors. The source of focusing is at midpoint 0 and traveltime 20ms. Two views are provided for a better perception of the tridimensional surface. nick2-feavo_data [CR]

dence of the polarity of the "V"s on the sign of the velocity anomaly.[3] This will have important consequences on the choice of FEAVO removal strategies, treated in a separate section towards the end of this paper.

FEAVA effects in the image

Simple algebraic manipulations of Equation 1 show that in Angle-Domain Common Image Gathers (ADCIGs), for constant velocity and flat reflectors, the shape of the FEAVA path is given by

$$z = z_a + |m - m_a| \cot\theta, \tag{2}$$

where z is depth, z_a is the depth of the heterogeneity, m is midpoint, m_a is the location of the anomaly, and θ is the reflection angle (Vlad, 2002). Figure 6 plots this surface. The "Kjartansson V's" are visible in the Grand Isle dataset after a $v(z)$ survey-sinking migration. Figure 7 shows two depth slices through the prestack image. The number of "V"s is particularly large in this dataset, making it less than suitable for isolating and studying a FEAVO instantiation free from interference. In a less crowded area of the figure, the circled upside-down "V" shows vertical continuity as well as borders of polarity opposite from that of the main image, as predicted by finite-frequency wave theory (Spetzler et al., 2004). Another property of data-domain FEAVO that gets carried over in the image domain is the dependence of the polarity of the effects on the sign of the velocity "lenses" (Figure 9). The effects along the described paths have a finite width, as exemplified by Figure 9. In the case of velocity-caused

[3] Assuming that one-way modeling produced morphologically correct effects – see more in the Modeling section.

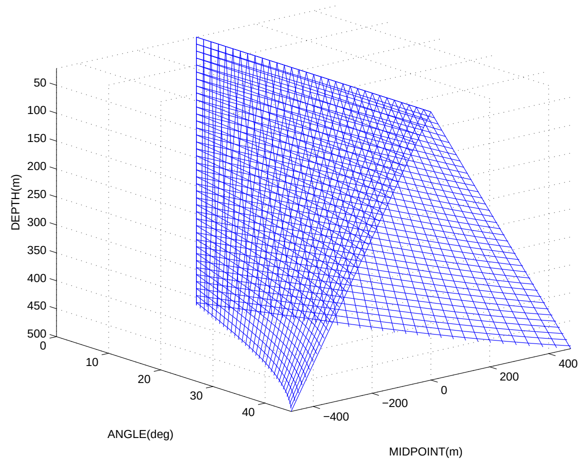

Figure 6: FEAVO path in ADCIGs, constant velocity, flat reflectors, heterogeneity 20m deep. Unlike in the data domain, the shape keeps on opening with depth and the arms of the "V's" are slightly curved. nick2-feavo_imag [CR]

FEAVO, the width of the path is linked to both the magnitude and the size of the heterogeneity. It is not known to what extent there is a magnitude-size ambiguity in the case of absorption. For both cases it may be possible to put an upper bound on the spatial extent of the anomaly based on the width of the FEAVO path, and this can be used as regularization in inversion for the anomalies or as an aid in interpretation.

Needed: A study of the link between the magnitude (intensity) and size (spatial extent) of the FEAVO source and the width of the FEAVA effects. This applies to data-domain effects too.

Migration removes any focusing effects which did not send energy outside the survey aperture (Vlad, 2005), so it will be easier to study FEAVA effects in the image than in the data – there is simply much less misplaced energy to interfere with the object of study.[4] To properly view (and extract) FEAVA, one must first resolve the background velocity well enough that there is no residual first-order curvature in ADCIGs. FEAVA effects, being caused by anomalies much smaller than the cable length, will manifest themselves as slight traveltime wiggling accompanied by high/low amplitudes. Figure 9 shows a synthetic example obtained of FEAVA effects "in a pure state", after all non-FEAVA energy has been removed.

The advantage of having less clutter in the image can be easily negated by a treatment of the data that emphasizes lack of noise over amplitude preservation. A comparation of Figure 2 in Vlad (2002) and Figure 6 in Vlad and Biondi (2002) shows an example of such an occurence. Using an amplitude-preserving processing and imaging flow is critical for correctly imaging the effects. Smearing the FEAVO effects with amplitude-careless processing is not removing them, but sweeping the dirt under the rug, since this will result in undesired FEAVO energy contaminating now unknown areas. Also, FEAVO removal may need to take into account the physics of the phenomenon, which need to be preserved. Vlad et al. (2003b) and Vlad and Tisserant (2004) describe the implementation of an amplitude-preserving shot-profile migration. The processing done before migration needs to use amplitude-preserving algorithms too.

[4]Multiples can be more of a problem, though.

Needed: A study of the amplitude properties of the offset-to-angle transformation used in creating the ADCIGs, and in particular the role of the regularization ϵ, the variation of which has been observed to have significant results.

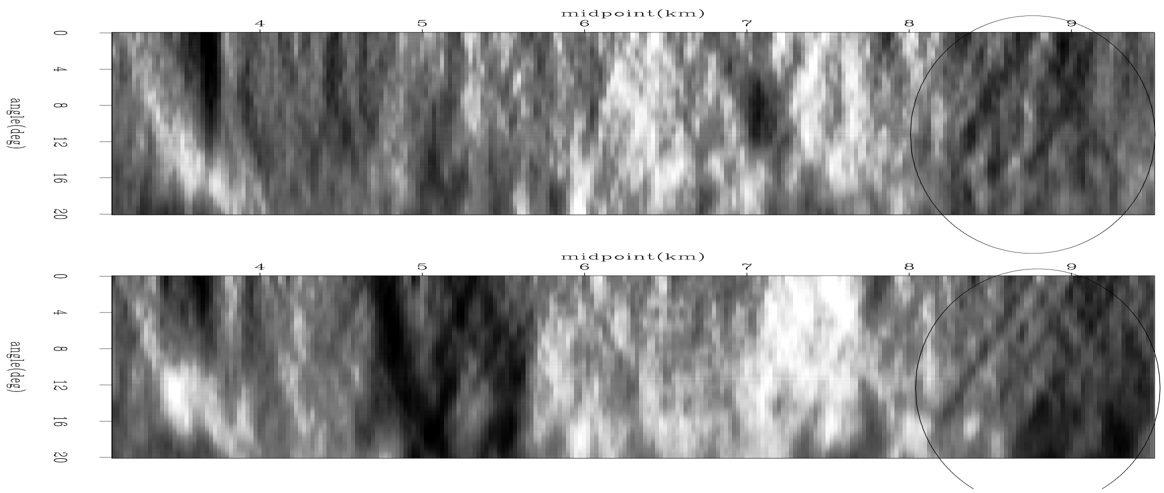

Figure 7: Depth slices 2.36km (top), 2.43km (bottom). Notice: (1) the slight opening of the upside-down, encircled "V" with depth, like in Figure 6; (2) its opposite-polarity borders; and (3) the rectangular shaded areas spanning all angles which may denote "legitimate", reflector-caused AVO if reflectors are flat enough in this area. nick2-apslim [CR]

An important point to note is that there is no relationship whatsoever between amplitude variations caused by focusing and those caused by variation of incidence angle on the reflector (FEAVO vs. "legitimate" AVO). The total amplitude of a reflector will show a superposition of the two effects, but the effects are physically independent from each other. *FEAVO effects do not obey the* sin^2 *dependence between amplitude and reflection angle given by Shuey (1985).* Figure 10 offers an illustration of this property, and the "FEAVO detection" and "FEAVO removal" sections explore its the applications.

FEAVO MIGRATION AND MODELING

Since velocity heterogeneities of the size of those which cause FEAVO break the high-frequency assumption of the ray theory (Woodward, 1990), wavefield extrapolation methods should be used to migrate and model FEAVO-affected data. Vlad (2005) has demonstrated qualitatively that one-way migration methods with the *correct* velocity model (containing the FEAVO-causing velocity lenses) eliminate all FEAVA effects from the image. The same publication shows in the same way that: (1) only FEAVO effects modeled with two-way schemes have a microstructure (i.e., width of the bordering shadows) identical to that of real data, but (2) the errors introduced by one-way modeling schemes are removed when migrating with one-way schemes *and the correct velocity model*. Thus the numerical experiments from Vlad et al.

(2003a), which show that migration with the correct velocity model removes FEAVA, keep their validity.

Needed: Mathematical proof of the conclusions of Vlad (2005), and further investigation for cases involving absorption.

Figure 8 shows the output of modeling FEAVO with a one-way scheme. While the synthetic dataset does feature the small traveltime anomalies associated with FEAVO, it does not exhibit the several-fold increase in amplitudes noticed in the real data and which got FEAVO discovered in the first place (Kjartansson, 1979; White et al., 1988). The magnitude of the velocity “lenses” (10% of the background) should have been sufficient to have caused it. It is unclear to what extent the lack of strong amplitude effects is caused by modeling with a one-way scheme in general (as discussed above) or by the amplitude characteristics of the particular one-way scheme employed. FEAVA effects obtained by modeling with a one-way scheme followed by migrating with the background velocity (Figure 9 have neither border shadows/highs as real data does (Figure 7), nor extremely high amplitudes. Modifications of the downward propagation operators designed to take into account vertical gradients in velocity (Vlad et al., 2003b) will not result in improvements in this case because the background velocity is constant. Having correct amplitudes of FEAVA effects, including their microstructure, is paramount to the success of any inversion-based removal procedure that inverts FEAVA into velocity/absorption anomalies, and any such procedure would need to be tested on a synthetic while being prototyped.

Needed: Extraction of “pure”, *correct* FEAVA effects by two-way modeling of FEAVA effects followed by two-way migration with the correct velocity, with the background velocity, and subtraction in ADCIGs. A comparison with the result of the equivalent one-way flow (Figure 9) will allow then to assess whether the errors introduced by the one-way problem are negligible or not.

Not only primaries are focused by the heterogeneities that caused FEAVO. Multiples are too. Vlad (2004a) uses numerical experiments on highly realistic data to present evidence towards the idea that, unlike FEAVO from primaries, FEAVO from multiples is not eliminated through simple migration that does not take multiples into account. It is easy to understand this intuitively: during a migration designed for primaries, the multiples wavefields do not pass through the focusing heterogeneities enough times for the focusing to be undone by the extrapolation operators. Another type of FEAVO that may not be eliminated by migration is the one caused by absorption. An absorption compensating-scheme, such as Lu et al. (2004), would need to be employed to eliminate FEAVO after an absorption model has been obtained through inversion.

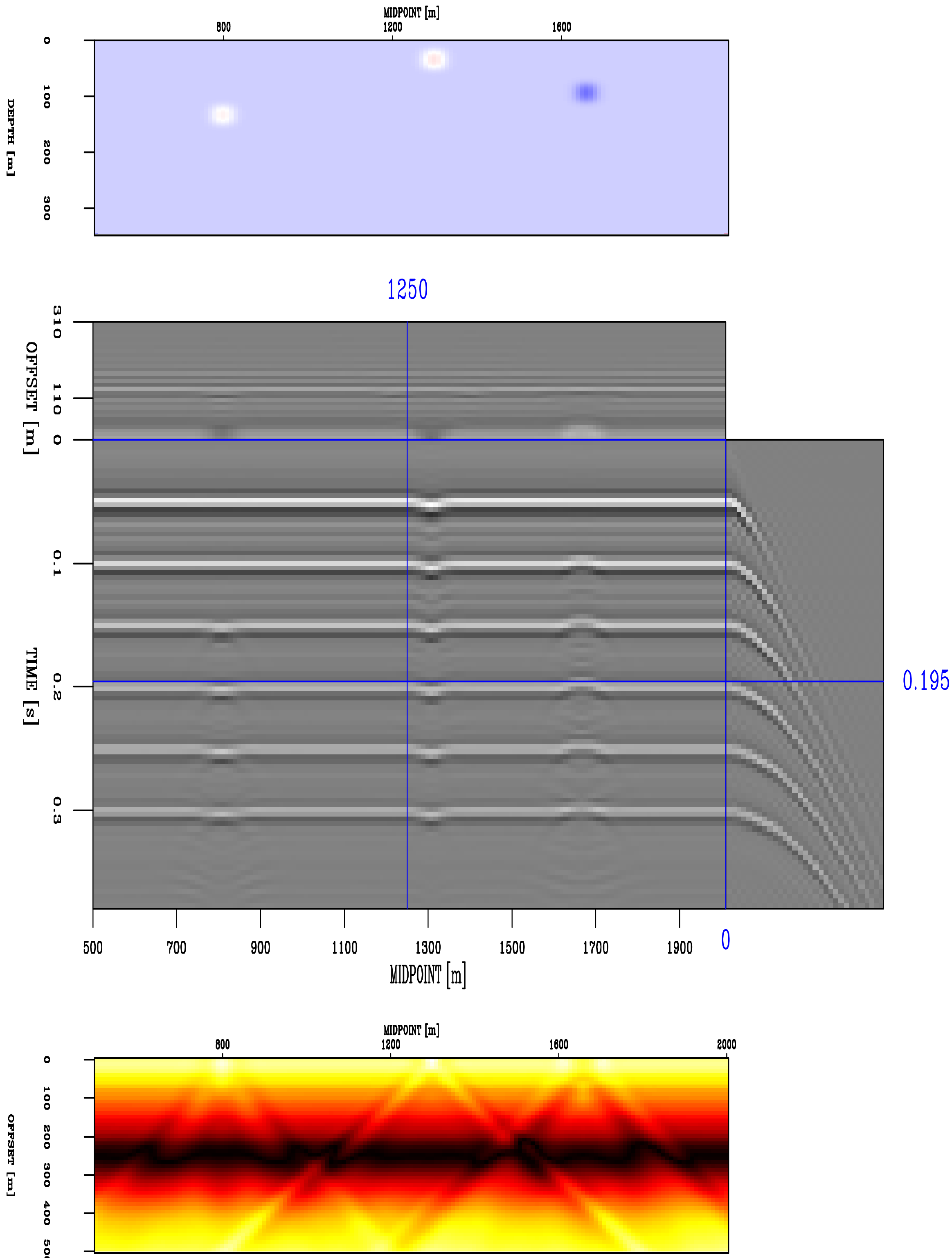

Figure 8: **Top:** Velocity model with 2000m/s background and anomalies with peak values, from left to right, of -153m/s, -188m/s and +231 m/s. **Middle:** Prestack data generated with one-way source-receiver upward continuation with two reference velocities. **Bottom:** "Kjartansson V's". From Vlad et al. (2003a). nick2-f1 [CR]

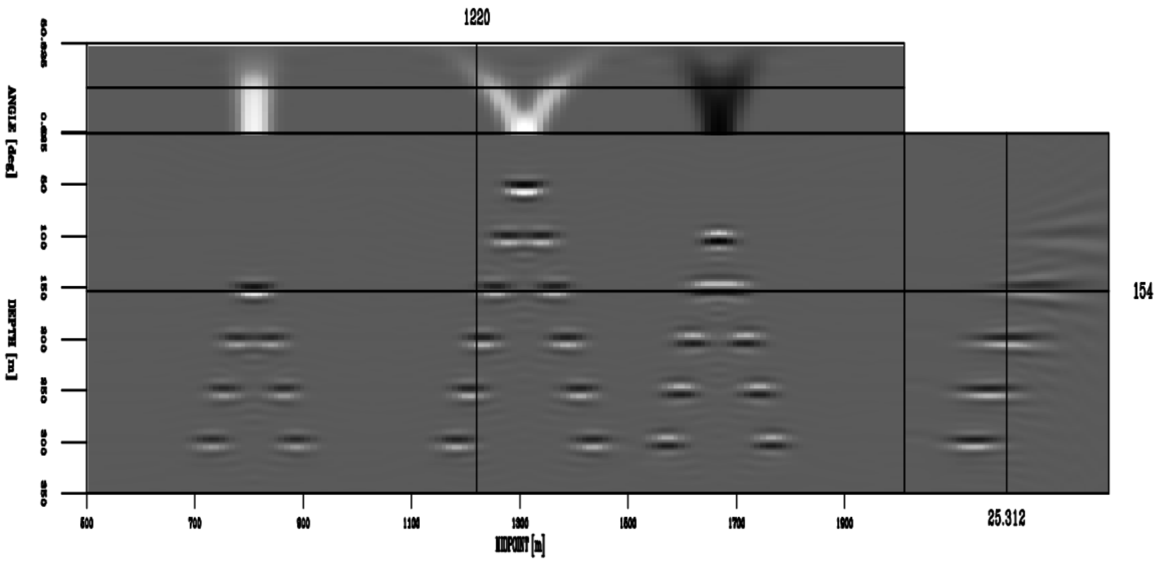

Figure 9: "Pure" FEAVA. Obtained by: (1) migrating the dataset shown in Figure 8 with the correct velocity; (2) migrating it with the background velocity; (3) subtracting the ADCIGs. From Vlad et al. (2003a). nick2-f6_top [CR]

FEAVA DETECTION

In order to remove FEAVO/FEAVA, or at least not to trust the amplitudes from the affected areas, one must be alerted to its existence. Visual inspection of zero-offset data for subvertical streaks of high energy provides a cue only in the case of the most powerful effects. "Kjartansson V's" would provide a good diagnostic tool if it were not for today's prestack data volumes which size in the terrabytes. Comparing stacks of near and far offsets is a good way of alerting that something is wrong (Hatchell, 2000a), but it does not highlight FEAVO specifically. Laurain et al. (2004) give a good way of quantitatively estimating the amplitudes due solely to propagation effects for a single reflector at a time. This method is even more labor-intensive than visually examining the prestack lines for "V"s. The worst one is to rely on the interpreter to realize if "something is wrong with the AVO" - he may just interpolate an intercept and gradient through the erratic values. What is needed is a quick, simple and robust way to signal the corruption of AVO by focusing.

Vlad (2004b) provides such a FEAVA detection method. The method is based on the fact that reflector-caused AVA for incidence angles $\theta < 30°$ is very well described (Shuey, 1985) by

$$R(\theta) = I + G\sin^2(\theta), \tag{3}$$

where I and G depend only on the lithology at the reflector. If the amplitudes are picked at a single midpoint-depth location not affected by focusing and plotted as a function of the $\sin^2(\theta)$, the values will arrange close to a line with intercept I and gradient G. The presence of FEAVO causes the linear dependence to break, as exemplified on a simple synthetic in

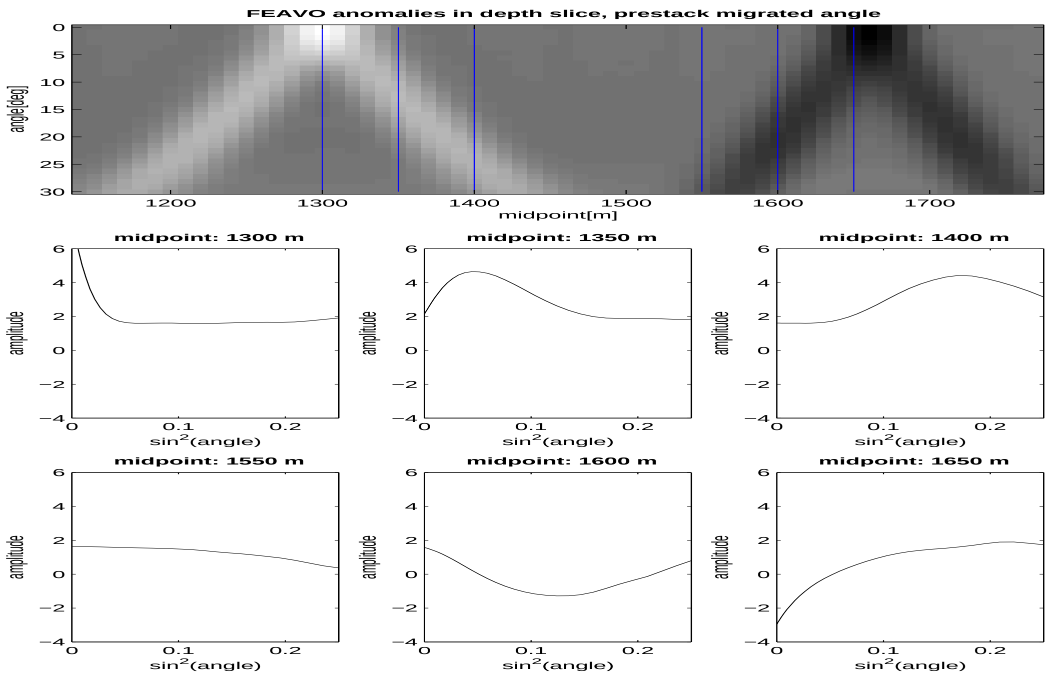

Figure 10: **Top panel:** Midpoint-angle depth slice from the prestack migrated synthetic dataset shown in Figure 9. From Vlad et al. (2003a). **Bottom panels:** Amplitudes at midpoints marked by vertical thin lines in the upper panel. From Vlad (2004b). nick2-examine_FEAVO [CR]

Figure 10. A direct estimate of the amount of FEAVA energy present at a (midpoint, depth) location can be obtained by measuring how much nonlinearity is in the dependence between amplitudes and $\sin^2(\theta)$. Simply interpolating a linear trend, subtracting it and computing the variance of the residual (Figure 11) provides a computationally cheap procedure with no knobs to turn. The "FEAVO attribute" output by this detector is "poststack-sized", having no offset dimensions and no intensive human labor requirement for the visual examination. The vertical clustering of the affected areas in clusters under the source anomalies helps with the detection and possibly with the interpretation of the heterogeneities that cause FEAVA as well. Figure 12 shows a simple example obtained by migrating with the background velocity the synthetic dataset from Figure 8. The FEAVO effects are very visible – everything that is certainly not FEAVO has been eliminated. By contrast, when looking for vertical streaks or Kjartansson "V"s in the data without the help of the detector, the eye is distracted by the very large amount of amplitudes that cannot possibly be FEAVO, but are still in the picture. Figure 13 shows that the FEAVO detector functions well in a complex case, with subtle (2-3% variation from the background) velocity "lenses" which produce barely visible subvertical high amplitude streaks in the stack. The robustness of the FEAVO detector is confirmed by its behavior in the presence of multiples. In Figure 14 multiples are also weakly highlighted, but they are not vertically correlated like FEAVO and therefore they are not a serious source of noise.

The output of the detector could be improved in principle by subtracting an interpretation-based estimation of the lithology-caused AVO, instead of just the best fitting line. However,

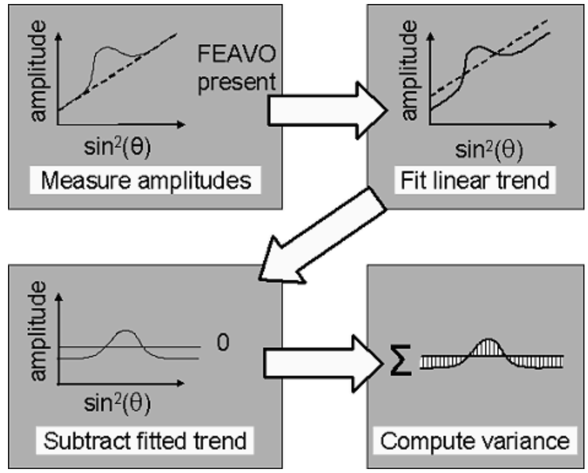

Figure 11: FEAVA detection flowchart. From Vlad and Biondi (2004). nick2-detect [NR]

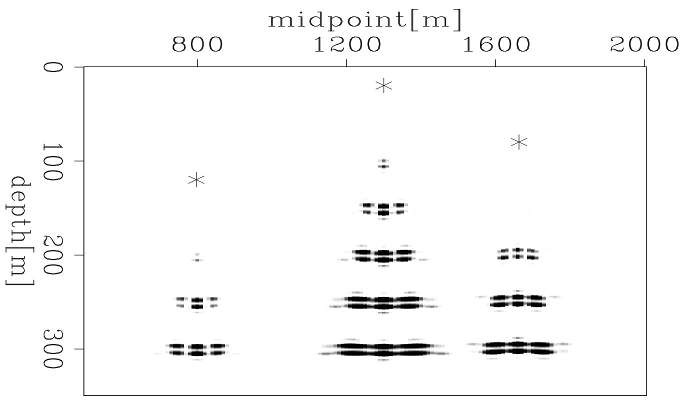

Figure 12: FEAVO anomalies flagged in the midpoint-depth space by the automatic detection procedure. The stars denote the location of the heterogeneities causing the focusing. From Vlad (2004b). nick2-anoloc [CR]

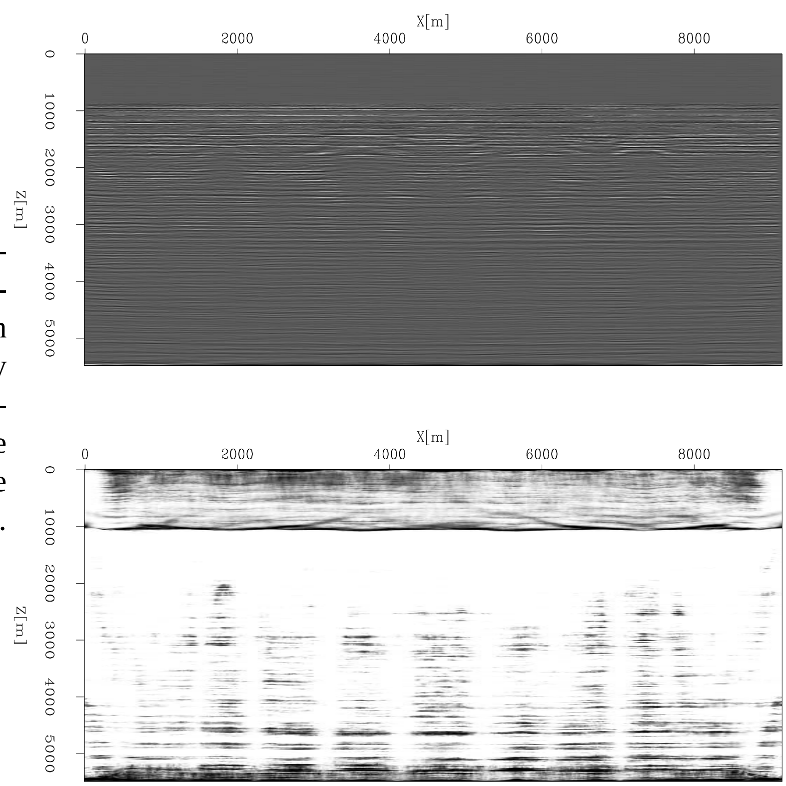

Figure 13: The FEAVO detector performs well on realistic data. Notice how barely visible focusing in the stack (top panel) is amplified by the detector (bottom panel). The erratic values in the upper part of the detector output are from above the sea bottom. From Vlad (2004a). nick2-com_nomult_imag [CR]

this would introduce complexity, expense and sources of errors for marginal gains. Simple as it is, the FEAVO detector works well independently for each midpoint, even when the rock-caused AVO is unknown, and even in the presence of multiples or limited aperture angles (Vlad, 2004a). A significant increase in complexity appears to be necessary, however, when trying to remove FEAVO from the data, which is the subject of the next section.

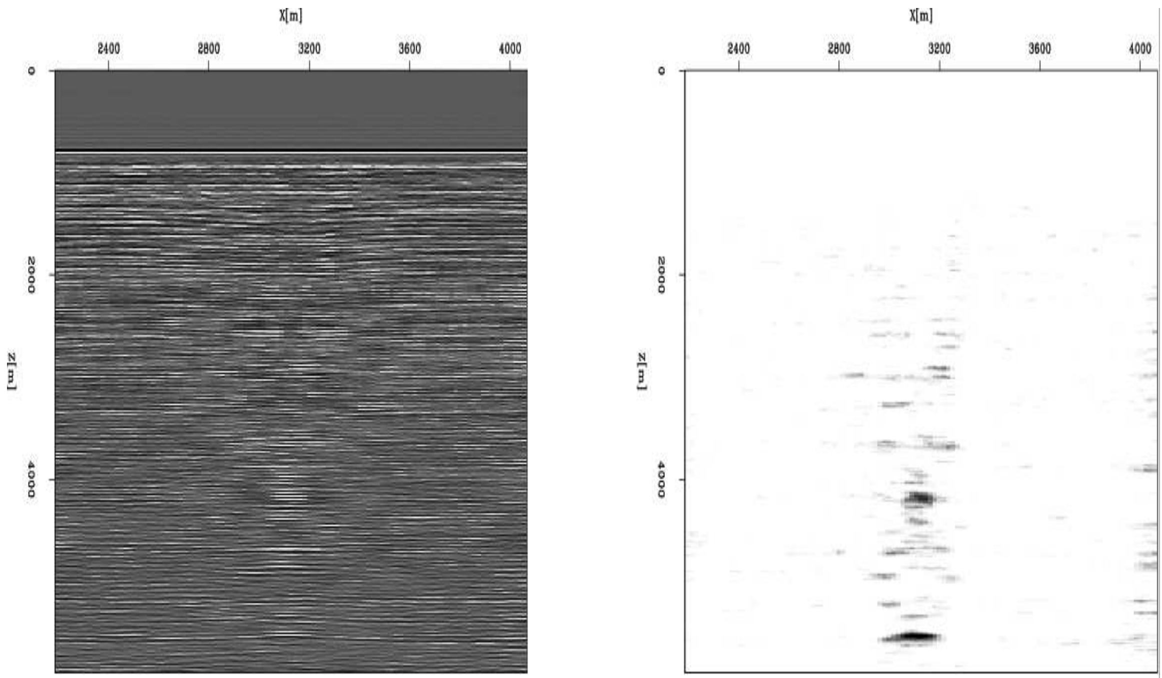

Figure 14: **Left:** $V(z)$ migration of FEAVO-affected data with internal multiples. The streak of energy in the center is barely visible. **Right:** Applying the FEAVO detector really highlights the focusing effects. From Vlad (2004a). nick2-bg-refvel1top2 [CR]

FEAVA REMOVAL

No approach attempted up to date has managed to successfully remove all FEAVA effects from ADCIGs. Hatchell (2000a) states that AVO stack (croscorrelate traces to get rid of the traveltime aspects of FEAVA, then stack) is effective in eliminating FEAVA from the stacked image. This, however, does not solve the problem of "contaminated" angle gather amplitudes which impedes AVA analysis.

Another avenue of approach consists of using the physics of FEAVO to generate a velocity/absorption anomaly section, and then to use it for imaging, which will eliminate FEAVO. Woodward (1987), Claerbout (1993), Bevc (1994), and Harlan (1994) follow the template laid out by Kjartansson (1979): (1) Generate a bidimensional midpoint-offset map of FEAVO effects as expressed in either the traveltime or the amplitude of unmigrated data. (2) Obtain the transmission anomaly section by inputting the map obtained at step 1 into an inverted operator. At first sight, the tomographic seismic amplitude correction in Harlan (1994) appears quite successful, managing to eliminate the FEAVO effects along particular well-defined reflectors one at a time by computing transmission anomaly sections used to correct the amplitudes. Nevertheless, he states that the transmission anomaly sections generated for different reflectors appear inconsistent, and that simultaneous inversion did not improve things. For "cleaning" the FEAVO effect the process must be repeated for each particular reflector, and it involves picking, a process prone to errors in the case of weaker reflectors. Most of these approaches suffered because of using ray theory, and all of them because they were working in the data domain, before migration eliminates other propagation effects. Also, none of them used all the FEAVO characteristics described in a previous section at the same time. Since this information is not redundant, all is necessary to properly characterize the FEAVO sources.

Vlad and Biondi (2002), Vlad (2002) and Vlad et al. (2003a) propose an approach that follows the strategy of finding a correct velocity model and imaging with it to get rid of FEAVO. Vlad (2004b) refine it further. This method proceeds as follows:

(1) Find the background velocity sufficiently well to flatten the ADCIGs, except for FEAVA effects.

(2) Perform prestack depth migration and transformation to ADCIGs.

(3) Process the ADCIGs so that in the end they contain *only* FEAVA effects, in the manner of Figure 9. Areas where no focusing effects are present are zeroed. In areas where FEAVA is overimposed with "legitimate", lithological AVA (everywhere else), the lithological AVA is found and subtracted, so that only FEAVA effects remain. The processed ADCIGs are called a "image perturbation".

(4) The image perturbation is transformed from ADCIGs to offset, fed into the adjoint of wavefield-extrapolation migration, then becomes input for inverse linearized downward continuation. The end product is a velocity update.

(5) The velocity field is updated and a new iteration proceeds.

This is an adaptation of Wavefield-Extrapolation Migration Velocity Analysis (WEMVA), an iterative inversion method described by Sava (2004). Figure 15 provides a flowchart. In essence, WEMVA linearizes and inverts the whole process of transforming a dataset and a velocity model into ADCIGs.

This is a complex machinery which invites several questions. What can go wrong? How large are the errors introduced by the inverse linearized downward continuation? Vlad et al. (2003a) explore in detail the answers. Provided an optimal image perturbation (with the help of a synthetic dataset), WEMVA manages to produce velocity updates that eliminate FEAVO from the ADCIGs through migration. The only step left to accomplish is extracting the FEAVA-only image perturbation.

Vlad (2004b) deals specifically with this issue. The (revised since then) FEAVA extraction process from the ADCIGs consists of the following steps:

(1) Detect: Use the FEAVA detector to keep all that can possibly be FEAVA. Set a threshold and zero the rest of the values in the ADCIGs.

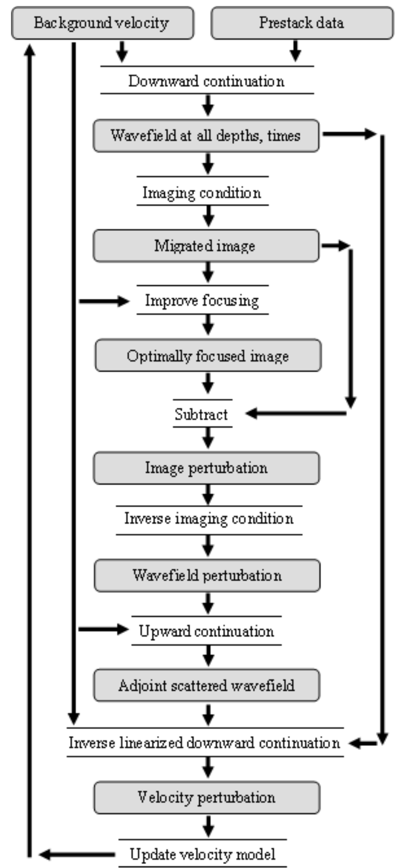

Figure 15: WEMVA flowchart. From Vlad and Tisserant (2004). nick2-wemva [NR]

(2) Focus: Take the absolute value/envelope of the output of (1) and run a weighed summation operator along precomputed velocity-dependent FEAVA surfaces. Semblance will not work because it will be attracted by higher coherence along the reflectors. The summation weights will consider the finite spatial extent of the FEAVA effects and may be negative in the exterior according to the extent of the bright/dim zones predicted by theory.

(3) Filter the output of (2) in the manner of Harlan (1986) to keep only the high semblance values.

(4) Spread back along the FEAVA surfaces, with weights, to obtain a weighted mask that indicates the probability of FEAVA presence in any voxel in ADCIGs. Zero everything in ADCIGs outside the mask.

(5) Interpolate reflector-caused lithological AVO inside the mask from values outside the mask and geologic information.

(6) Subtract the output of (5) from the corresponding unaltered values in ADCIGs at the respective locations.

Needed: a working implementation of the image perturbation extraction process described above.

FEAVA effects are a suitable input for WEMVA because the small traveltime effects makes them satisfy easily the Born approximation required from WEMVA inputs. There are variations of WEMVA which are not subject to the Born constraints (Sava and Symes, 2002), but they incorporate the image perturbation extraction step inside the inversion process, making it difficult to isolate errors that may appear during the design and prototyping of the FEAVA extraction procedure described above.

WEMVA coupled with FEAVA extraction in the manner described above has many strengths that previous approaches did not have. It considers every aspect of FEAVO, it uses wavefield-extrapolation methods, and it takes the input of the inversion from the image domain. Potential weaknesses lay in the subjectivity associated with the image perturbation extraction, with the cost (each linear solver iteration contains a prestack downward continuation and a prestack upward continuation; several solver iterations are required for a single step of WEMVA.) and with the fact that it does not consider absorption, which is likely to exist in real data.

CONCLUSIONS

This paper represents itself the conclusions of seven other papers on this topic over a period of three years. The work presented here is by no means finished. On the contrary, the main purpose of this paper was to collect in a single place the most meaningful information in order to allow a strategic view on the FEAVO problem. I believe that any physics-based approach to FEAVA removal needs first a solid foundation of knowledge about the characteristics of the phenomenon, especially in the image domain. This will allow building proper FEAVA extraction tools. No reason why WEMVA-based FEAVA removal should not work has been identified. In the past three years the amount of information on all aspects of the FEAVO problem has increased and I expect that to happen in the future.

ACKNOWLEDGMENTS

I thank Biondo Biondi for guidance and to Paul Sava for meaningful discussions. I thank Guojian Shan for the pseudospectral wave propagation code used in Figure 2. I thank Dr. Ralph Shuey of Gulf Science and Technology Company for making the Grand Isle dataset used in Figure 3 available to SEP (1978). I thank ChevronTexaco for providing the synthetic velocity model used for Figures 13 and 14 and the dataset in Figure 14.

REFERENCES

Bevc, D., 1994, Datuming velocity from traveltime tomography: SEP–**82**, 145–164.

Bortfeld, R., 1961, Approximations to the reflection and transmission coefficients of plane longitudinal and transverse waves: Geophys. Prosp., **09**, no. 04, 485–502.

Carazzone, J. J., Eriksen, E. A., and Rokhlin, V., 1984, Connection between phase and amplitude for the acoustic wave equation:, *in* 54th Ann. Internat. Mtg Soc. of Expl. Geophys. Expanded Abstracts, 738–740.

Claerbout, J. F., 1993, Reflection tomography: Kjartansson revisited: SEP–**79**, 59–68.

Craft, C., 1973, Detecting hydrocarbons: For years the goal of exploration geophysics: Oil and Gas Journal, **Feb. 19**.

Gutenberg, B., 1936, The amplitudes of waves to be expected in seismic prospecting: Geophysics, **01**, no. 02, 252–256.

Harlan, W. S., 1986, Signal-noise separation and seismic inversion: Ph.D. thesis, Stanford University.

Harlan, W. S., 1994, Tomographic correction of transmission distortions in reflected seismic amplitudes: Soc. Expl. Geophys, 64th Annual Internat. Mtg., Soc. Expl. Geophys., Expanded Abstracts, 968–971.

Hatchell, P., 1999, Fault whispers: Transmission distortions on prestack seismic reflection data: Soc. Expl. Geophys, 69th Annual Internat. Mtg., Soc. Expl. Geophys., Expanded Abstracts, 864–867.

Hatchell, P., 2000a, Fault whispers: Transmission distortions on prestack seismic reflection data: Geophysics, **65**, no. 2, 377–389.

Hatchell, P., 2000b, What causes distortions on prestack reflection seismic data?: World Oil, **221**, no. 11, 69–77.

Kjartansson, E., 1979, Analysis of variations in amplitudes and traveltimes with offset and midpoint: SEP–**20**, 1–24.

Laurain, R., Vinje, V., and Strand, C., 2004, Simulated migration amplitude for improving amplitude estimates in seismic illumination studies: The Leading Edge, **23**, no. 03, 240–245.

Lu, R., Lovell, R., DawsonII, D., and Yu, Y., 2004, Compensation of the gas-cap attenuation with viscoacoustic wave-equation migration: A case study from west africa:, *in* 74th Ann. Internat. Mtg. Soc. of Expl. Geophys., 476–477.

Rocca, F., and Toldi, J., 1982, Lateral velocity anomalies: SEP–**32**, 1–14.

Sava, P., and Symes, W. W., 2002, A generalization of wave-equation migration velocity analysis: SEP–**112**, 27–36.

Sava, P., 2004, Migration and velocity analysis by wavefield extrapolation: Ph.D. thesis, Stanford University.

Sheriff, R. E., and Geldart, L. P., 1995, Exploration Seismology: Cambridge University Press.

Shuey, R. T., 1985, A simplification of the Zoeppritz equations: Geophysics, **50**, no. 4, 609–614.

Spetzler, J., Jocker, J., Smeulders, D., and Trampert, J., 2004, Validation of first-order wave diffraction theory by an ultrasonic experiment:, *in* 74th Ann. Internat. Mtg. Soc. of Expl. Geophys., 2180–2183.

Stephens, R. B., and Sheng, P., 1985, Acoustic reflections from complex strata: Geophysics, **50**, no. 7, 1100–1107.

Vlad, I., and Biondi, B., 2002, Velocity estimation for seismic data exhibiting focusing-effect avo: SEP–**111**, 107–123.

Vlad, I., and Biondi, B., 2004, Velocity estimation for seismic data exhibiting focusing-effect AVO: Soc. of Expl. Geophys., Expanded Abstracts, 2427–2430.

Vlad, I., and Tisserant, T., 2004, Improving the amplitude accuracy of downward continuation operators (part 2): SEP–**115**, 81–88.

Vlad, I., Biondi, B., and Sava, P., 2003a, Velocity estimation for seismic data exhibiting focusing-effect AVO (part 3): SEP–**114**, 101–110.

Vlad, I., Tisserant, T., and Biondi, B., 2003b, Improving the amplitude accuracy of downward continuation operators: SEP–**113**, 163–176.

Vlad, I., 2002, Velocity estimation for seismic data exhibiting focusing-effect avo (part 2): SEP–**112**, 47–64.

Vlad, I., 2003, Frequency-dependent velocity analysis?: SEP–**114**, 119–124.

Vlad, I., 2004a, The influence of multiples and imaging approximations on focusing-effect AVA detection and removal: SEP–**117**, 95–104.

Vlad, I., 2004b, Velocity estimation for seismic data exhibiting focusing-effect avo (part 4): SEP–**115**, 265–272.

Vlad, I., 2005, Migration and modeling of seismic data affected by focusing-effect AVO/AVA: SEP–**120**, 317–322.

White, B. S., Nair, B., and Bayliss, A., 1988, Random rays and seismic amplitude anomalies: Geophysics, **53**, no. 07, 903–907.

Woodward, M., 1987, Reflection tomography : Vees in midpoint offset space: SEP–**51**, 1–12.

Woodward, M., 1990, Wave equation tomography: Ph.D. thesis, Stanford University.